Title Page

The title of the paper

4-Nonylphenol induces disruption of spermatogenesis associated with oxidative stress-related apoptosis by targeting p53-Bcl-2/Bax-Fas/FasL signalling

The short title

4-nonylphenol induces reproductive toxicity in male rats

The full names of the authors

Peng Duan[1], Chunhui Hu[2], Holly J. Butler[3], Chao Quan[1], Wei Chen[1], Wenting Huang[1], Sha Tang[1], Wei Zhou[1], Meng Yuan[1], Yuqin Shi[4] , Francis L. Martin[3] & Kedi Yang*[1]

Affiliations of authors

[1]*MOE (Ministry of Education) Key Lab of Environment and Health, Department of Occupational and Environmental Health, Tongji Medical College, Huazhong University of Science and Technology, Wuhan 430030, China;*

[2]*Department of Laboratory Medicine, Taihe Hospital, Hubei University of Medicine Shiyan 442000, Hubei, China;*

[3]*Centre for Biophotonics, Lancaster Environment Centre, Lancaster University, Bailrigg, Lancaster LA1 4YQ, UK;*

[4]*Department of Epidemiology and Health Statistics, School of Public Health, Medical College, Wuhan University of Science and Technology, Wuhan 430030, China*

***Corresponding author:** Department of Occupational and Environmental Health, Tongji Medical College, Huazhong University of Science and Technology, 13 Hangkong Road, 430030 Wuhan, Hubei Province, China. Tel: +86-0278-3693897; Fax: +86-0278-3657765; E-mail: yangkd@mails.tjmu.edu.cn (Kedi Yang)*

Number of tables and figures

2 Tables and 9 Figures

References

56

Main text

6800 words (including references)

Quantity of Supporting Information

1 Supplementary Table and 1 Supplementary Figure

4-Nonylphenol induces disruption of spermatogenesis associated with oxidative stress-related apoptosis by targeting p53-Bcl-2/Bax-Fas/FasL signalling

ABSTRACT: 4-Nonylphenol (NP) is a ubiquitous environmental chemical with estrogenic activity. Our aim was to test the hypothesis that pubertal exposure to NP leads to testicular dysfunction. Herein, twenty four seven-week-old rats were randomly divided into four groups and treated with NP (0, 25, 50 or 100 mg/kg body weight every 2 days for 20 consecutive days) by intra-peritoneal injection. Compared to untreated controls, the parameters of sperm activation rate, curvilinear velocity, average path velocity and swimming velocity were significantly lower at doses of 100 mg/kg, while sperm morphological abnormalities were higher, indicating functional disruption and reduced fertilization potential. High exposure to NP (100 mg/kg) resulted in disordered arrangement of spermatoblasts and reduction of spermatocytes in seminiferous tubules, whilst tissues exhibited a marked decline in testicular fructose content and serum FSH, LH and testosterone levels. Oxidative stress was induced by NP (50 or 100 mg/kg) as evidenced by elevated MDA, decreased SOD and GSH-Px, and inhibited antioxidant gene expression (*CAT*, *GPx*, *SOD1* and *CYP1B1*). In addition, NP treatment decreased proportions of Ki-67 positive cells and increased apoptosis in a dose-dependent manner. Rats treated with 100 mg/kg NP exhibited significantly increased mRNA expression of caspase-1, -2, -9 and -11, decreased caspase-8 and PCNA1 mRNA expression, down-regulation of Bcl-2/Bax ratios and up-regulation of Fas, FasL and p53 at the protein and mRNA levels. Taken together, NP-induced apoptosis, hormonal deficiencies and depletion of fructose potentially impairs spermatogenesis and sperm function. p53-independent Fas/FasL-Bax/Bcl-2 pathways may be involved in NP-induced oxidative stress-related apoptosis.

Keywords: apoptosis; endocrine disruptor; 4-Nonylphenol; oxidative stress; spermatogenesis; testicular dysfunction

INTRODUCTION

The xenoestrogen 4-nonylphenol (NP) is the final degradation product of nonylphenol polyethoxylates (NPEOs) (Krupinski et al., 2014). NP is regarded to be an endocrine disrupting chemical (EDC), which could be involved in declines in semen quantity and quality observed amongst adult men (Schiffer et al., 2014; Tohyama et al., 2015). With the extensive usage of NPEOs in the preparation of domestic, agricultural and industrial products, large amounts of NP have been released into various mediums of water environments (Corada-Fernandez et al., 2013; Fan et al., 2013). Thus, NP was found in 62 source water samples from 31 major cities across China with median and maximum concentrations of 123 and 918 ng/L, respectively (Fan et al., 2013). Median concentrations of NP in drinking water were 27 ng/L in China (Fan et al., 2013) and 20 ng/L in United States (Padhye et al., 2014). Previous studies have established that NP is common in food, including fish, animal tissues, milk, cereals, vegetables and fruits (Fan et al., 2013; Niu et al., 2015). Due to its lipophilic properties and long half-life, the metabolite NP is bioaccumulated by aquatic organisms and humans (Riva et al., 2010). NP's contamination and toxicity poses a potential hazard to human health and development.

Spermatogenesis is affected by a combination of endocrine, environmental and/or genetic factors (Juul et al., 2014). There is increasing evidence that NP is detrimental to various organs, including testis (Yuan et al., 2013). Specifically, multiple studies show NP inhibition of spermatozoa motility and viability *in vitro* (Lukac et al., 2013; Shao et al., 2011; Uguz et al., 2015). I*n vivo* studies confirm such *in vitro* observations in exhibiting reduced sperm counts and motility, incomplete testicular descent, testicular mal-development, seminiferous tubule degeneration, and abnormal sperm morphology (Aly et al., 2012; Ye et al., 2012). Although some animal studies suggest NP-induced spermatotoxicity and spermatogenesis failure, the reproductive effects of this agent remains obscure and further studies are warranted to confirm its adverse effects on various sperm motility parameters.

A prominent effect of EDCs is the induction of oxidative stress (Tavares et al., 2016). Oxidative stress-mediated testicular dysfunction is an important pathological mechanism underlying male infertility (Wan et al., 2013). Some studies have suggested that NP administration increases levels of lipid peroxidation and oxidative stress in testis, which were correlated with altered germ cell development and reproductive function (Aly et al., 2012; Chitra et al., 2002; Lu et al., 2014). Moreover, enhanced oxidative stress results in DNA, protein or lipid damage, inducing apoptosis (Klaunig et al., 2010). In addition, NP has the potential to induce cytotoxicity and apoptosis in Sertoli cells (SC) and Leydig cells (LC), which compromises reproductive outcomes (Choi et al., 2014; Wu et al., 2009; Ying et al., 2012). Pre-pubertal exposure to NP caused testicular dysfunction by increasing levels of apoptotic testicular germ cells (Han et al., 2004; Yao and Hou, 2004). The precise causal relationship between NP-induced oxidative stress and activation of apoptotic signalling pathways *in vivo* is still poorly understood.

The goal of this study was to investigate the adverse reproductive effects of NP on male rats exposed during puberty. Sperm parameters, reproductive hormones, fructose content, oxidative stress and antioxidant gene expression were determined. We then examined the potential role of NP in proliferation inhibition and apoptosis induction of different testicular cell populations, and explored the involvement of mitochondrial and death receptor pathways in NP-induced apoptosis.

MATERIALS AND METHODS

Chemicals and Reagents

4-Nonylphenol (Mixture of isomers; CAS no. 84852-15-3; empirical formula C15H24O; molecular meight 220.35) with 99% analytical standard was purchased from ACROS Organics (Leicestershire, UK). Follicle-stimulating hormone (FSH) immunoradiometric assay kits and luteinizing hormone (LH) radioimmunoassay kits were purchased from MP Biochemicals (Asse-Relegem, Belgium). The testosterone assay kit, fructose assay kit, malondialdehyde (MDA), glutathione peroxidase (GSH-Px) and superoxide dismutase (SOD) kits were obtained from Nanjing Jiancheng Bioengineering Institute (Nanjing, China). TRIzol® Reagent and Platinum® SYBR® Green qPCR SuperMix-UDG kit was purchased from Invitrogen (Carlsbad, CA). Revert Aid First Strand cDNA Synthesis kit was purchased from Fermentas UAB (Vilnius, Lithuania). DeadEnd™ Fluorometric TUNEL System kit was purchased from Promega (Madison, WI, USA). Polyclonal rabbit antibody against Ki-67 was purchased from Abcam (Cambridge, MA, USA). BCA protein assay kit, Western and IP cytolysis were purchased from Beyotime Company of Biotechnology (Shanghai, China). Rabbit monoclonal antibodies against p53, Bcl-2, Bax, Fas and FasL were purchased from Cell Signalling Technology (Cambridge, MA, USA). Secondary antibody (horseradish peroxidase-labelled goat anti-rabbit) was purchased from Amersham Pharmacia Biotech (Buckinghamshire, UK).

Animals and Treatment

The experimental protocol was approved by the Institutional Animal Care and Use Committee of the Tongji Medical College (IACUC protocol number: 373). All procedures were carried out in accordance with the approved guidelines of institutional animal ethics committee.

Twenty-four Sprague-Dawley (SD) rats (male, 6-week-old), cleaning grade, were purchased from Tongji Medical College Animal Center (Wuhan, China), and were housed in a controlled animal room (room temperature: 22-25℃; relative humidity: 45-60%). Dark: light cycles were maintained at a 12-h day-night cycle. Each animal had access *ad libitum* to purified water and standard rodent chow.

After 1 week of acclimatization, 7-week-old rats were randomly separated into four groups of 6 rats each: three NP treatment groups and a vehicle control group. The no-observed-adverse-effect level of NP on reproductive capacity was reported as 10-50 mg/kg/day in rats (Nagao et al., 2001). Moreover, NP at 100 mg/kg/d or greater can exert toxicity to epididymis and testis (Aly et al., 2012; Lu et al., 2014). So we selected the dose of 25, 50 and 100 mg/kg for use in this study. In NP-treated groups, the rats were exposed to NP dissolved in corn oil by intra-peritoneal injection at doses of 25, 50 or 100 mg/kg body weight per 2 days. Vehicle control rats were injected with equal volumes of corn oil. The rats were treated for 20 consecutive days. The injection volume of each dose was 10 ml/kg body weight and rats were weighed immediately prior to treatment to calculate the actual volume of administration.

Collection of Blood and Tissue Samples

After NP treatment, the rats were weighed and sacrificed by decapitation. Blood samples were taken from the eye and were allowed to coagulate for 2 h at 4℃ before being centrifuged at

3000 rpm for 10 min. Serum was analysed immediately or stored at -80℃ until analysis.

The testis and other reproductive organs were quickly removed, weighed and rinsed immediately with ice-cold physiological saline (0.9% NaCl) and stored at -80°C until biochemical determinations were made (within 1 month). The dissected tissue (5×5×3 mm) of each left testis was fixed in 4% paraformaldehyde buffer, processed, embedded in paraffin for haematoxylin-eosin (H&E) staining, terminal deoxynucleotidyl transferase-mediated, labelling (TUNEL) analysis and Ki-67 immunostaining. The dissected tissue (2×2×2 mm) of each right testis was fixed in 2.5% glutaraldehyde for electron microscopic observations. The remaining tissues from the bilateral testes were frozen by immersion in liquid nitrogen and stored at -80℃ until biochemical analysis.

Sperm Density, Motility and Malformation Rate

The left epididymis was used for evaluation of sperm parameters. After decapitation, cauda epididymis and ductus deferens were dissected immediately, trimmed of residual fat, rinsed briefly in pre-warmed physiological saline (37℃) and then placed in a small petri dish with 2 ml sperm nutrient solution. Ten deep cuts were made along the proximal and distal cauda of each epididymis and incubated at 37℃ in a 95% air and 5% CO_2 humidified incubator for 2 min. After that, a sperm suspension (5 µl) was taken onto a clean glass slide and computer-assisted semen analysis (CASA) was used to detect sperm count, motility and motion parameters.

The right epididymis was used for routine sperm deformation test. A routine sperm deformation test was conducted according to a previously described method (Quan et al., 2014). Under the microscope, 400 sperm were observed in each rat. Sperm morphology was categorised into normal/abnormal, the abnormalities were further classified into: multiple heads, multiple tails, irregularly shaped tail and head. The frequency of abnormal sperm was expressed as percentage, calculated using the following formula: [number of abnormal sperm ÷ total number of normal and abnormal sperm scored] ×100.

Estimation of Fructose and Hormone Levels

Serum concentrations of FSH, LH and testosterone were measured by double-antibody ELISA methods according to the standard protocol supplied by the kit manufacturer. The contents of fructose and protein in each testes were determined according to methods described in the references using commercial kits. All samples and standards were measured in triplicate.

Testicular Histopathology

Four-µm-thick sections were obtained from paraffin blocks using a rotatory microtome. Next sections were mounted on a microscope slide, stained with H&E, and then examined under a fluorescence microscope (Olympus, Tokoy, Japan) according to standard protocols.

Determination of Antioxidant Enzyme Activities and MDA Levels

Serum antioxidant enzyme activities of MDA, SOD and GSH-Px, level of MDA and activities of SOD and GSH-Px in testis tissue were measured with the corresponding detection kit according to the manufacturer's instructions. Notably, testicular tissues were decapsulated and homogenized in RIPA lysis buffer. The supernatant was collected for the assays of enzyme activities and protein content. The protein in supernatant samples was quantified by the method of BCA following the

manufacturer's instructions. The absorbance measured by a microplate reader (BIO-RAD). The enzyme activity was calculated and expressed per mg protein (Wang et al., 2015; Yao et al., 2015).

Transmission Electron Microscopy

Small testicular specimens were fixed in 2.5% glutaraldehyde, dehydrated, embedded in Eponate-12 overnight. Ultrathin sections were stained with 1% uranyl acetate and 1% lead citrate. The ultrastructural characteristics of germinal cells were observed and photographed using a Tecnai G2 12 Transmission electron microscopy (FEI Company, Holland). The experiment was repeated twice.

Proliferation and TUNEL Assays

Ki-67 staining was performed for determination of cell proliferation. Paraffin-embedded testis sections (4-μm thickness) were incubated with antibodies against Ki-67. After three washes, sections were incubated with fluorophore-conjugated secondary antibody for 1 h, and subsequently 4'-6-diamidino-2-phenylindole. Apoptosis was evaluated by the TUNEL assay. Four-μm-thick sections were stained using DeadEndTM Fluorometric TUNEL System following the vendor's recommendations. After additional nuclear staining with DAPI, the coverslips (for Ki-67 and TUNEL assessment) were mounted on slides with fluorescence mounting medium. The samples were visualized using a fluorescence microscope, and photomicrographs taken using a digital camera. For Ki-67 and TUNEL staining (green fluorescence), nuclei were quantified. For each section, four seminiferous tubules were counted for total number of nuclei *versus* nuclei positively stained in green. Ki-67 index and apoptotic index were expressed as the percentage change [100%×(number of positive nuclei/total number of nuclei)]. These analyses were performed in two sections from each rat.

Real-Time Quantitative RT PCR

Total RNA was extracted with Trizol reagents according to the manufacturer's protocol. Primer sequences used for real-time RT-PCR analysis are summarized in Table S1. Equal amounts of RNA (2 μg) were reverse transcribed using Revert Aid First Strand cDNA Synthesis Kit. RT-PCR was performed with an ABIPRISM® 7900HT Sequence Detection System (Applied Biosystems) using Platinum® SYBR® Green qPCR SuperMix-UDG with ROX. *β-actin* is regarded as a housekeeping gene. Qualitatively comparisons were made by the intensity ratio between target gene and *β-actin*.

Western Blot Analysis

Testicular tissues were prepared by lysing in RIPA lysis buffer and homogenizing. Debris was removed and protein content was quantified using the BCA Protein assay kit according to the manufacturer's instructions. Protein samples (20 μg per lane) were separated by electrophoresis on sodium dodecyl sulfate (SDS) polyacrylamide gels and transferred to nitrocellulose membranes by electroblotting. The membranes were blocked in 5% nonfat milk in Tris buffered saline (TBS) containing 0.05% Tween 20 (TBST) for 2 h at room temperature and probed with primary antibodies overnight at 4℃. The membranes were then washed with four changes of TBST and incubated with the appropriate horseradish peroxidase-conjugated secondary antibodies for 1 h at room temperature. Finally, after three more rinses with TBST, the immuno-reactive protein bands

were visualized by ECL exposure to X-ray film. Densitometric analysis was performed on scanned images of blots using Quantity One software.

Statistical Analysis

Results were expressed as the means ± SD from at least three independent experiments. The statistical analysis was performed by *t*-text and one-way analysis of variance using SPSS software version 12.0 (SPSS Inc., Chicago, IL, USA). $P < 0.05$ and $P < 0.001$ were considered as significant or very significant, respectively.

RESULTS

Effect of NP on Testis Weight

No deaths were observed in any group. As shown in Fig. S1, there were no significant differences in initial body weights, final body weights, body weight gain or testicular weights, as well as the weight coefficient of testis among the groups ($P > 0.05$).

Effects of NP on Sperm Functional Characteristics and Morphology

The changes in sperm characteristics of rats treated with NP are summarized in Table 1. Sperm activation rate was significantly decreased by 10.62% and 14.62% in response to treatment with NP (50 or 100 mg/kg, respectively) ($P < 0.01$). The 100 mg/kg NP exposure caused significant decreases in VCL, VAP and A&B grade sperm count as compared to vehicle control ($P < 0.05$). Moreover, the abnormal sperm morphology rates were significantly higher in the groups that received 50 or 100 mg/kg NP than in the vehicle control group ($P < 0.01$). Furthermore, five different abnormalities (including coiled or bent tails, tailless form, conjoined sperm with double heads and double tails, coiled or bent heads, and no-hook head) in sperm morphology were observed (Fig. 1).

Effects of NP on Reproductive Hormones and Fructose

The plasma levels of FSH, LH and testosterone were significantly decreased in 100 mg/kg NP-treated rats when compared with the control ($P < 0.05$, Fig. 2A,B,C). Administration of NP (50 or 100 mg/kg) dramatically decreased the levels of fructose in fresh testes ($P < 0.01$, Fig. 2D) as compared with vehicle controls. These results indicate that testicular utilisation of fructose by spermatozoa and hormonal balances were seriously affected.

NP-induced Testicular Histopathological Changes

Histological appearances of testicular tissues of control and NP-treated groups are shown in Fig. 3. The histo-architecture of the testis from control rats reveal a normal morphology and structure, consisting of well-organized seminiferous tubules with the successive stages of spermatogenesis and normal interstitial connective tissue. In contrast, testes from rats treated with 50 or 100 mg/kg NP exhibit seminiferous tubule degeneration characterised by disorganized, shrunken tubules with irregular, buckled basement membranes and incomplete spermatogenesis. Notably, some seminiferous tubules in the 100 mg/kg group were virtually devoid of spermatids and sperm.

Effects of NP on Oxidative Stress

Comparatively, our results show that inducing rats with NP (50 or 100 mg/kg) results in significant reductions in the activities of SOD and GSH-Px in testicular tissue, while MDA

content was significantly increased ($P < 0.05$, Fig. 4A). Similarly, serum SOD and GSH-Px activities were significantly decreased and serum MDA levels were significantly elevated in 50 and 100 mg/kg NP groups compared with the control group ($P < 0.05$, Fig. 4B). Furthermore, mRNA levels of SOD1, CAT, GPx and CYP1B1 were significantly decreased in response to NP treatment (100 mg/kg) as compared to the control ($P < 0.05$, Fig. 5).

Ultrastructural Alterations in Testicular Tissues

The fine structure of testicular cells is shown in Fig. 6. In controls, cytoplasmic organelles and nuclei of SC, LC and spermatogenic cells appear normal, along with normal-looking mitochondria with cristae. After NP administration (50 or 100 mg/kg), most of abnormalities were found in spermatogonia (SPG) (Fig. 6A), SC (Fig. 6B), LC (Fig. 6C), primary spermatocyte (SPT) (Fig. 6D) and secondary SPT (Fig. 6E). Morphological characteristics of apoptosis, such cytoplasmic shrinkage (SC, LC and SPT), condensed or marginated chromatin (LC and SPT), nuclear debris (secondary SPT), aggregation and swelling of mitochondria with loss of cristae appearing as vacuolated mitochondria (SPG, SC and SPT) were observed. Ultrastructural characteristics of spermatids at different stages are shown in Fig. 6F,G,H. No differences in the fine structure of spermatids and sperm were seen in testes taken from controls and rats treated with NP (50 or 100 mg/kg).

Effects of NP on Rates of Apoptosis and Proliferation in Spermatogenic Cells

Detected by TUNEL staining (Fig. 7A), NP exposure increased levels of apoptotic testicular cells from $5.46 \pm 1.06\%$ (50 mg/kg) to $6.33 \pm 1.68\%$ (100 mg/kg). Compared with control ($1.52 \pm 0.28\%$), levels of TUNEL-positive cells were significantly elevated ($P < 0.01$). Also, anti-Ki67 immunohistochemistry revealed that the majority of Ki67-positive cells were SPG, primary SPT and spermatids in the control group (Fig. 7B). Percentages of Ki67-positive cells in the 50 and 100 mg/kg NP-treated group ($15.23 \pm 4.52\%$ and $14.52 \pm 5.16\%$, respectively) were significantly lower than in controls ($37.73 \pm 8.14\%$) ($P < 0.01$). Moreover, RT-PCR analysis revealed that NP treatment (100 mg/kg) significantly decreased *PCNA1* mRNA levels in comparison with controls (Table 2).

NP Induces Mitochondrial-mediated and Death Receptor−mediated Apoptosis

As shown in Table 2, RT-PCR identified NP-induced caspase activation in testicular tissue. Levels of caspase-1, -2, -9 and -11 mRNA were considerably elevated and caspase-8 was significantly down-regulated in the 100mg/kg NP group in comparison with controls (all $P < 0.05$), suggesting caspase activation during apoptosis. Furthermore, significant reductions in mRNA expression levels of anti-apoptotic Bcl-xl and Bcl-2 were observed following 100 mg NP/kg. Meanwhile, we observed a significant up-regulation of pro-apoptotic Bax and Bad, p53, Fas and FasL mRNA in both 50 and 100 mg NP/kg groups. Likewise, the protein levels of Bax, Fas, FasL and p53 were significantly increased after 100 mg/kg NP administration ($P < 0.01$), whilst the Bcl-2 protein level was markedly down-regulated ($P < 0.01$), as shown by Western blot (Fig. 8A) and quantification analysis (Fig. 8B).

DISCUSSION

The oestrogen-like actions of NP have been implicated in causing testicular impairments (Yuan et al., 2013). Herein, we observed that NP disrupted spermatogenesis and caused spermatotoxic effects such as hormone deficiency, fructose depletion, oxidative stress and testicular cell

apoptosis, consequently impairing sperm function in adult rats. More importantly, NP exposure impacted on testicular cell fate by the modifying of p53, Fas/Fasl and Bcl-2/Bax signalling.

To examine the effects of NP on male fertility, we hypothesised that NP adversely affects male reproductive function through decreasing sperm quantity and motility, thus reducing fertilization rate. However, no changes in quantity or quality of epididymal sperm were found after NP administration, suggesting correct sperm maturation during transit in the epididymis. Sperm motility parameters are useful when evaluating quality and fertilizing potential (Giribabu et al., 2014; Perobelli et al., 2012). Herein, the surprising finding was that NP administration resulted in a significant decrease in activated sperm, VSL, VCL and swimming velocity; meanwhile, amplified sperm morphology abnormalities, indicating the induction of spermatotoxicity (deteriorated sperm function and morphology) (Ito et al., 2014). Alterations in motility parameters may cause an inefficient sperm penetration of cervix mucus, impairing the ability of sperm to reach the oocyte as well as penetrate through the zona pellucida (Fernandez et al., 2011; Jiang et al., 2011). Since a high percentage of sperm with progressive motility is related to a high fertilization index (Celik-Ozenci et al., 2011; Fernandez et al., 2011), such detrimental impacts on motility parameters induced by NP would seriously diminish sperm-fertilizing capacity. Moreover, observed regressive histopathological changes in the seminiferous tubules indicate that NP disturbs spermiogenesis, which is well supported by the observed degeneration of seminiferous tubules and spermatogenesis. Together, these observations indicate that NP can trigger testicular functional deterioration, stimulating us to further investigate its mechanism.

Studies have highlighted that development and maintenance of spermatogenesis is critically dependent upon the pituitary hormone FSH and androgens locally produced in response to LH (O'Shaughnessy 2014). FSH acts to stimulate spermatogonial proliferation and entry into meiosis (Mihalik et al., 2015). LH is as effective as FSH in maintaining spermatogenesis (O'Shaughnessy 2014). Both LH and FSH, secreted by the anterior pituitary, can stimulate LC and SC and, in turn, boost the secretion of testosterone from LC. Testosterone is the key hormone responsible for regulating spermatogenesis (Dirican and Kalender, 2012), together with maintaining the blood-testis barrier and, supporting the completion of meiosis and spermiation (Mihalik et al., 2015). Importantly, fructose synthesis and secretion is dependent upon the secretion of testosterone (Sharma et al., 2013). As noted above, optimal spermatogenesis is a result of the comprehensive effect of hormonal regulation. We show that 100 mg NP/kg significantly reduces plasma FSH and LH levels. Meanwhile, a remarkable decline in testosterone secretion and fructose production is observed in NP-treated (50 and 100 mg/kg) rats. Consequently, NP exposure is associated with the changes in hormonal status and spermatogenesis. NP-induced deficiencies of hormone and fructose potentially contribute to sperm dysfunction and aberrant spermatogenesis.

It is interesting to note that the testis is a major target organs for oxidative stress owing to its high levels of polyunsaturated membrane lipids (Ghabili et al., 2009). Based on the fact that NP-induced oxidative stress has been previously reported (Chitra et al., 2002; Choi et al., 2014), we suggest that oxidative stress is involved in NP-induced male reproductive toxicity. Herein, NP stimulates oxidative stress, characterized by an increase in lipid peroxidation (MDA) and a decrease in antioxidant enzymes (SOD and GSH-Px). There was also a significant reduction in expression of antioxidant genes (*CAT*, *GPx*, *SOD1* and *CYP1B1*) that was observed in the 100

mg/kg NP group. It has been reported that increased oxidative stress leads to antioxidant responses that involve modulation of the activity of antioxidant enzymes (Madhubabu and Yenugu 2014), further supporting our findings. Of note, sperm cells as well as sperm plasma membrane contain very high proportions of polyunsaturated fatty acids (PUFA) (Yan et al., 2013). PUFA are positively correlated with sperm function and semen quality and are particularly susceptible to oxidative stress (Henkel, 2011; Uygur et al., 2014; Yan et al., 2013). Therefore, we propose that metabolic bioactivation of NP triggers oxidative damage resulting in deterioration of semen parameters.

A considerable body of evidence suggests a direct connection between testicular oxidative stress and degenerated seminiferous tubules (Li et al., 2010; Nirupama et al., 2013). Disrupted oxidant-antioxidant balance results in oxidative stress, and consequently apoptosis and germ cell depletion (Nirupama et al., 2013). It is notable that apoptosis plays an important role in the induction of testicular toxicity. Caspase cascades are involved in oxidative stress-mediated apoptosis (Anselmi et al., 2007). This is evident herein, as ultrastructural changes confirm the appearance typical of apoptosis amongst LC, SC and spermatogenic cells. Also, the apoptotic index increased in the NP-treated group as previously noted (Choi et al., 2014; Jubendradass et al., 2012). Notably, the expression of caspase-1, -2, -8, -9 and -11 mRNA were activated by NP administration (100 mg/kg), indicating that spermatogenic and androgenic processes are possibly influenced by the oxidative damage-evoked apoptosis. In contrast, decreases in Ki67 and PCNA1 expression in testicular germ cells indicate a reduction in proliferative activity and spermatogenesis. Hormonal balance can be severely influenced by testicular germ cell apoptosis, specifically by LG and SC (Aksglaede et al., 2006; Itman et al., 2015). The absence of LG and SC secretory function is detrimental to spermatogenesis and spermatozoa (Itman et al., 2015). Thus we speculate that NP-induced toxicity in male reproduction probably depends on an imbalance between proliferation and apoptotic cell death in testis.

To further explore the molecular mechanism of NP-induced apoptosis, two major pathways for caspase activation were explored, including the death receptor-induced extrinsic pathway and the mitochondria-mediated apoptotic intrinsic pathway. *Bcl-2* and *Bax* of the Bcl-2 gene families are central to the regulation of mitochondrial apoptosis (Dai et al., 2015). There is evidence that the ratio of Bcl-2/Bax determines the dichotomous point in cells towards triggered apoptosis (Rengarajan et al., 2014). The best-characterized extrinsic apoptotic pathway is that mediated by the surface molecule Fas/FasL system (Jubendradass et al., 2012). Furthermore, it has been demonstrated that p53 can function as a master regulator of the apoptotic framework, capable of coordinating the cell-intrinsic and -extrinsic apoptotic signalling cascades (Maheshwari et al., 2009; Yang et al., 2015). Consistent with previous studies (Jubendradass et al., 2012; Sabbieti et al., 2011), we found that 100 mg NP/kg markedly down-regulates Bcl-2/Bax ratio, up-regulates the protein and mRNA expression of Fas, FasL and p53, compared with control. Under certain conditions, oxidative stress triggers the p53 response, which could transactivate downstream target genes (such as *Bax*, *Bcl-2*, *Fas* and *FasL*) and apoptosis (Gali-Muhtasib et al., 2015; Yang et al., 2015). In this contextn, one can suppose that NP-induced testicular cell apoptosis is partially related to p53-associated Bcl-2/Bax and Fas/FasL death-signalling pathways. Such molecular mechanisms underlying NP-induced death signal transduction and simultaneous activation of the intrinsic pathways in the presence of p53 require further investigation.

Conclusion

In conclusion, our results present *in vivo* evidence demonstrating that NP interferes with male fertility as evidenced by sperm dysfunction, severe sperm morphological abnormalities and, histological and ultrastructural impairments of seminiferous tubules. In addition, suppression of hormone secretion, inhibition of testicular fructose production, oxidative imbalance and apoptosis may disrupt spermatogenesis leading to NP-related male reproductive disorder. In particular, induction of apoptosis in testis is correlated with the p53/Fas/Bax signalling pathways. This is schematically summarized in Fig. 9. Our results may shed light on the pathogenesis of infertility and provide insights into the relationship between NP exposure and testicular dysfunction. However, the complete molecular mechanisms underlying NP-induced testicular apoptosis need to be further investigated.

Acknowledgments

Conflict of Interest

The Authors did not report any conflict of interest.

References

Aksglaede L, Wikstrom AM, Rajpert-De Meyts E, Dunkel L, Skakkebaek NE, Juul A. 2006. Natural history of seminiferous tubule degeneration in Klinefelter syndrome. Hum Reprod Update 12: 39-48.

Aly HA, Domenech O, Banjar ZM. 2012. Effect of nonylphenol on male reproduction: analysis of rat epididymal biochemical markers and antioxidant defense enzymes. Toxicol Appl Pharmacol 261: 134-141.

Anselmi K, Stolz DB, Nalesnik M, Watkins SC, Kamath R, Gandhi CR. 2007. Gliotoxin causes apoptosis and necrosis of rat Kupffer cells in vitro and in vivo in the absence of oxidative stress: exacerbation by caspase and serine protease inhibition. J Hepatol 47: 103-113.

Celik-Ozenci C, Tasatargil A, Tekcan M, Sati L, Gungor E, Isbir M, et al. 2011. Effects of abamectin exposure on male fertility in rats: potential role of oxidative stress-mediated poly(ADP-ribose) polymerase (PARP) activation. Regul Toxicol Pharmacol 61: 310-317.

Chitra KC, Latchoumycandane C, Mathur PP. 2002. Effect of nonylphenol on the antioxidant system in epididymal sperm of rats. Arch Toxicol 76: 545-551.

Choi MS, Park HJ, Oh JH, Lee EH, Park SM, Yoon S. 2014. Nonylphenol-induced apoptotic cell death in mouse TM4 Sertoli cells via the generation of reactive oxygen species and activation of the ERK signaling pathway. J Appl Toxicol 34: 628-636.

Corada-Fernandez C, Lara-Martin PA, Candela L, Gonzalez-Mazo E. 2013. Vertical distribution profiles and diagenetic fate of synthetic surfactants in marine and freshwater sediments. Sci Total Environ 461-462: 568-575.

Dai L, Han Y, Ma T, Liu Y, Ren L, Bai Z, et al. 2015. Effects of Deep Electroacupuncture Stimulation at "Huantiao" (GB 30) on Expression of Apoptosis-Related Factors in Rats with Acute Sciatic Nerve Injury. Evid Based Complement Alternat Med 2015: 157897.

Dirican EK, Kalender Y. 2012. Dichlorvos-induced testicular toxicity in male rats and the protective role of vitamins C and E. Exp Toxicol Pathol 64: 821-830.

Fan Z, Hu J, An W, Yang M. 2013. Detection and occurrence of chlorinated byproducts of bisphenol a, nonylphenol, and estrogens in drinking water of china: comparison to the parent compounds. Environ Sci Technol 47: 10841-10850.

Fernandez CD, Bellentani FF, Fernandes GS, Perobelli JE, Favareto AP, Nascimento AF, et al. 2011. Diet-induced obesity in rats leads to a decrease in sperm motility. Reprod Biol Endocrinol 9: 32.

Gali-Muhtasib H, Hmadi R, Kareh M, Tohme R, Darwiche N. 2015. Cell death mechanisms of plant-derived anticancer drugs: beyond apoptosis. Apoptosis 20: 1531-1562.

Ghabili K, Shoja MM, Agutter PS, Agarwal A. 2009. Hypothesis: intracellular acidification contributes to infertility in varicocele. Fertil Steril 92: 399-401.

Giribabu N, Kumar KE, Rekha SS, Muniandy S, Salleh N. 2014. Chlorophytum borivilianum (Safed Musli) root extract prevents impairment in characteristics and elevation of oxidative stress in sperm of streptozotocin-induced adult male diabetic Wistar rats. BMC Complement Altern Med 14: 291.

Han XD, Tu ZG, Gong Y, Shen SN, Wang XY, Kang LN, et al. 2004. The toxic effects of nonylphenol on the reproductive system of male rats. Reprod Toxicol 19: 215-221.

Henkel RR. 2011. Leukocytes and oxidative stress: dilemma for sperm function and male fertility. Asian J Androl 13: 43-52.

Itman C, Bielanowicz A, Goh H, Lee Q, Fulcher AJ, Moody SC, et al. 2015. Murine Inhibin alpha-Subunit Haploinsufficiency Causes Transient Abnormalities in Prepubertal Testis Development Followed by Adult Testicular Decline. Endocrinology 156: 2254-2268.

Ito Y, Tomizawa M, Suzuki H, Okamura A, Ohtani K, Nunome M, et al. 2014. Fenitrothion action at the endocannabinoid system leading to spermatotoxicity in Wistar rats. Toxicol Appl Pharmacol 279: 331-337.

Jiang JT, Sun WL, Jing YF, Liu SB, Ma Z, Hong Y, et al. 2011. Prenatal exposure to di-n-butyl phthalate induces anorectal malformations in male rat offspring. Toxicology 290: 322-326.

Jubendradass R, D'Cruz SC, Rani SJ, Mathur PP. 2012. Nonylphenol induces apoptosis via mitochondria- and Fas-L-mediated pathways in the liver of adult male rat. Regul Toxicol Pharmacol 62: 405-411.

Juul A, Almstrup K, Andersson AM, Jensen TK, Jorgensen N, Main KM, et al. 2014. Possible fetal determinants of male infertility. Nat Rev Endocrinol 10: 553-562.

Klaunig JE, Kamendulis LM, Hocevar BA. 2010. Oxidative stress and oxidative damage in carcinogenesis. Toxicol Pathol 38: 96-109.

Krupinski M, Janicki T, Palecz B, Dlugonski J. 2014. Biodegradation and utilization of 4-n-nonylphenol by Aspergillus versicolor as a sole carbon and energy source. J Hazard Mater 280: 678-684.

Li J, Wang Z, Shi D, Chen Y. 2010. Adult exposure to sasanguasaponin induces spermatogenic cell apoptosis in vivo through increased oxidative stress in male mice. Toxicol Ind Health 26: 691-700.

Lu WC, Wang AQ, Chen XL, Yang G, Lin Y, Chen YO, et al. 2014. 90d Exposure to Nonylphenol has Adverse Effects on the Spermatogenesis and Sperm Maturation of Adult Male Rats. Biomed Environ Sci 27: 907-911.

Lukac N, Lukacova J, Pinto B, Knazicka Z, Tvrda E, Massanyi P. 2013. The effect of nonylphenol on the motility and viability of bovine spermatozoa in vitro. J Environ Sci Health A Tox Hazard Subst Environ Eng 48: 973-979.

Madhubabu G, Yenugu S. 2014. Allethrin induced toxicity in the male reproductive tract of rats contributes to disruption in the transcription of genes involved in germ cell production. Environ Toxicol 29: 1330-1345.

Maheshwari A, Misro MM, Aggarwal A, Sharma RK, Nandan D. 2009. Pathways involved in testicular germ cell apoptosis induced by H2O2 in vitro. FEBS J 276: 870-881.

Mihalik J, Maslankova J, Solar P, Horvathova F, Hubkova B, Almasiova V, et al. 2015. The effect of R-(-)-deprenyl administration on reproductive parameters of rat males. Eur J Pharmacol 754: 148-152.

Nagao T, Wada K, Marumo H, Yoshimura S, Ono H. 2001. Reproductive effects of nonylphenol in rats after gavage administration: a two-generation study. Reprod Toxicol 15: 293-315.

Nirupama M, Devaki M, Nirupama R, Yajurvedi HN. 2013. Chronic intermittent stress-induced alterations in the spermatogenesis and antioxidant status of the testis are irreversible in albino rat. J Physiol Biochem 69: 59-68.

Niu Y, Zhang J, Duan H, Wu Y, Shao B. 2015. Bisphenol A and nonylphenol in foodstuffs: Chinese dietary exposure from the 2007 total diet study and infant health risk from formulas. Food Chem 167: 320-325.

O'Shaughnessy PJ. 2014. Hormonal control of germ cell development and spermatogenesis.

Semin Cell Dev Biol 29: 55-65.

Padhye LP, Yao H, Kung'u FT, Huang CH. 2014. Year-long evaluation on the occurrence and fate of pharmaceuticals, personal care products, and endocrine disrupting chemicals in an urban drinking water treatment plant. Water Res 51: 266-276.

Perobelli JE, Alves TR, Toledo FC, Fernandez CD, Anselmo-Franci JA, Klinefelter GR, et al. 2012. Impairment on sperm quality and fertility of adult rats after antiandrogen exposure during prepuberty. Reprod Toxicol 33: 308-315.

Quan C, Shi Y, Wang C, Wang C, Yang K. 2014. p,p'-DDE damages spermatogenesis via phospholipid hydroperoxide glutathione peroxidase depletion and mitochondria apoptosis pathway. Environ Toxicol.

Rengarajan T, Nandakumar N, Rajendran P, Haribabu L, Nishigaki I, Balasubramanian MP. 2014. D-pinitol promotes apoptosis in MCF-7 cells via induction of p53 and Bax and inhibition of Bcl-2 and NF-kappaB. Asian Pac J Cancer Prev 15: 1757-1762.

Riva C, Porte C, Binelli A, Provini A. 2010. Evaluation of 4-nonylphenol in vivo exposure in Dreissena polymorpha: Bioaccumulation, steroid levels and oxidative stress. Comp Biochem Physiol C Toxicol Pharmacol 152: 175-181.

Sabbieti MG, Agas D, Palermo F, Mosconi G, Santoni G, Amantini C, et al. 2011. 4-nonylphenol triggers apoptosis and affects 17-beta-estradiol receptors in calvarial osteoblasts. Toxicology 290: 334-341.

Schiffer C, Muller A, Egeberg DL, Alvarez L, Brenker C, Rehfeld A, et al. 2014. Direct action of endocrine disrupting chemicals on human sperm. EMBO Rep 15: 758-765.

Shao ZX, Jiang HT, Liang F, Zhu BC. 2011. [Effects of nonylphenol and cadmium on sperm acrosome reaction in vitro in mice]. Zhonghua Nan Ke Xue 17: 318-321.

Sharma V, Boonen J, Spiegeleer BD, Dixit VK. 2013. Androgenic and spermatogenic activity of alkylamide-rich ethanol solution extract of Anacyclus pyrethrum DC. Phytother Res 27: 99-106.

Tavares RS, Escada-Rebelo S, Correia M, Mota PC, Ramalho-Santos J. 2016. The non-genomic effects of endocrine-disrupting chemicals on mammalian sperm. Reproduction 151: R1-R13.

Tohyama S, Miyagawa S, Lange A, Ogino Y, Mizutani T, Tatarazako N, et al. 2015. Understanding the molecular basis for differences in responses of fish estrogen receptor subtypes to environmental estrogens. Environ Sci Technol 49: 7439-7447.

Uguz C, Varisli O, Agca C, Evans T, Agca Y. 2015. In vitro effects of nonylphenol on motility, mitochondrial, acrosomal and chromatin integrity of ram and boar spermatozoa. Andrologia 47: 910-919.

Uygur R, Aktas C, Tulubas F, Uygur E, Kanter M, Erboga M, et al. 2014. Protective effects of fish omega-3 fatty acids on doxorubicin-induced testicular apoptosis and oxidative damage in rats. Andrologia 46: 917-926.

Wan HT, Mruk DD, Wong CK, Cheng CY. 2013. Targeting testis-specific proteins to inhibit spermatogenesis: lesson from endocrine disrupting chemicals. Expert Opin Ther Targets 17: 839-855.

Wang FY, Liu JM, Luo HH, Liu AH, Jiang Y. 2015. Potential protective effects of Clostridium butyricum on experimental gastric ulcers in mice. World J Gastroenterol 21: 8340-8351.

Wu J, Wang F, Gong Y, Li D, Sha J, Huang X, et al. 2009. Proteomic analysis of changes induced by nonylphenol in Sprague-Dawley rat Sertoli cells. Chem Res Toxicol 22: 668-675.

Yan L, Bai XL, Fang ZF, Che LQ, Xu SY, Wu D. 2013. Effect of different dietary

omega-3/omega-6 fatty acid ratios on reproduction in male rats. Lipids Health Dis 12: 33.

Yang G, Zhang W, Qin Q, Wang J, Zheng H, Xiong W, et al. 2015. Mono(2-ethylhexyl) phthalate induces apoptosis in p53-silenced L02 cells via activation of both mitochondrial and death receptor pathways. Environ Toxicol 30: 1178-1191.

Yao G, Hou Y. 2004. Nonylphenol induces thymocyte apoptosis through Fas/FasL pathway by mimicking estrogen in vivo. Environ Toxicol Pharmacol 17: 19-27.

Yao Z, Zhang Y, Li H, Deng Z, Zhang X. 2015. Synergistic effect of Se-methylselenocysteine and vitamin E in ameliorating the acute ethanol-induced oxidative damage in rat. J Trace Elem Med Biol 29: 182-187.

Ye XF, Yao YF, Wang LZ. 2012. [Study on reproductive toxicity in male embryo rats with the pregnancy SD rates exposed by nonylphenol]. Zhonghua Lao Dong Wei Sheng Zhi Ye Bing Za Zhi 30: 856-858.

Ying F, Ding C, Ge R, Wang X, Li F, Zhang Y, et al. 2012. Comparative evaluation of nonylphenol isomers on steroidogenesis of rat Leydig Cells. Toxicol In Vitro 26: 1114-1121.

Yuan HX, Xu X, Sima YH, Xu SQ. 2013. Reproductive toxicity effects of 4-nonylphenol with known endocrine disrupting effects and induction of vitellogenin gene expression in silkworm, Bombyx mori. Chemosphere 93: 263-268.

TABLE I. Effect of 4-nonylphenol at different doses on sperm concentration, motility, motility parameters, and morphology

Parameters	4-nonylphenol (mg/kg body weight every 2 days)			
	0 (control)	25 mg/kg	50 mg/kg	100 mg/kg
Sperm density and motility				
Total counts	2180.17±676.43	2189.00±809.36	2466.33±597.67	2375.00±667.12
Total motility	1309.50±568.63	1491.67±559.43	1623.00±456.32	1529.17±532.78
Total density (millions/mL)	177.58±32.59	197.38±68.42	229.93±56.79	218.14±38.58
Activate rate (%)	74.68±5.60	69.41±5.51	66.75±3.00**	63.76±3.87**
Motile sperm density (millions/mL)	133.84±22.96	134.90±47.85	142.94±42.70	139.33±35.49
Motion parameters				
VCL (µm/s)	40.19 ±2.31	39.49±2.83	39.92±4.14	35.71±2.68*
VSL (µm/s)	22.58±4.50	21.55±2.36	22.23±4.73	20.03±4.47
VAP (µm/s)	29.40±2.27	27.12±2.37	26.32±2.97*	24.79±2.16**
Average ALH (µm)	5.43±0.61	5.25±0.39	5.10±0.56	4.91±0.83
Maximal ALH (µm)	14.62±1.31	14.75±1.13	14.54±1.37	13.93±2.00
Average BCF (times/s)	7.79±0.67	7.70±0.83	7.46±0.39	7.36±0.74
Rates of FP (%)	24.08±3.33	24.82±3.34	25.42±4.70	23.97±3.32
Density of FP (millions/ml)	50.71±20.20	50.36±20.57	55.58±18.92	53.19±15.7
Sperm swimming velocity				
Sperms of grade A (%)	28.61±4.01	24.32±5.12	24.60±7.89	20.49±6.28
Sperms of grade B (%)	18.61±2.73	17.01±1.36	14.74±1.38**	14.50±1.29**
Sperms of grade C (%)	21.17±2.96	26.42±4.00	27.41±7.53	28.44±5.24
Sperms of grade D (%)	31.61±3.78	32.26±3.05	33.26±2.25	36.57±2.92*
Sperms of grade A &B (%)	47.22±5.47	41.33±5.64	39.34±9.16	34.99±6.79**
Sperms of grade C &D (%)	52.78±5.47	58.67±5.64	60.66±9.16	65.01±6.79**
Sperm abnormalities				
Rates of teratosperm (%)	2.50±0.52	3.10±0.75	13.20±3.05**	11.50±2.73**

Abbreviations: VCL, curvilinear velocity; VSL, straight line velocity; VAP, average path velocity; ALH, amplitude of lateral head displacement; BCF, beat cross frequency; FP, sperm moving in forward linear motion called forward progression. The data are expressed as the mean ± SD for six animals per dose. *P <0.05, **P <0.01 *versus* 0 mg/kg group (Vehicle control).

TABLE II. Effects of 4-nonylphenol on mRNA levels of proliferation- and apoptosis-related genes of testicular tissue in rats

Gene	4-nonylphenol (mg/kg body weight every 2 days)			
	0 (control)	25 mg/kg	50 mg/kg	100 mg/kg
Proliferation marker				
PCNA1	1.08±0.17	1.16±0.13	1.09±0.21	0.86±0.14*
Caspase family				
Caspase 1	1.08±0.20	1.33±0.16*	1.34±0.17*	1.60±0.25**
Caspase 2	1.03±0.04	1.50±0.36*	1.94±0.56**	1.63±0.26**
Caspase 3	0.98±0.11	0.79±0.08*	0.98±0.19	1.16±0.23
Caspase 6	1.01±0.16	1.05±0.12	0.94±0.16	0.90±0.18
Caspase 7	1.06±0.13	0.87±0.22	0.92±0.16	1.08±0.17
Caspase 8	1.03±0.15	0.88±0.11	0.91±0.18	0.83±0.18*
Caspase 9	1.09±0.11	1.59±0.21**	1.67±0.21**	1.72±0.37**
Caspase 11	1.08±0.08	1.76±0.17**	2.06±0.22**	2.10±0.35**
Bcl-2 family				
Bad	1.07±0.13	1.45±0.27**	1.40±0.19**	1.43±0.11**
Bax	1.00±0.21	1.85±0.18**	1.87±0.19**	1.52±0.28**
Bcl-2	1.02±0.12	1.03±0.17	1.00±0.52	0.80±0.13*
Bcl-xl	1.06±0.09	0.62±0.14**	1.04±0.14	0.70±0.19*
p53-mediated mitochondrial and death receptor signalling				
p53	1.03±0.10	1.23±0.06*	1.25±0.22*	1.38±0.11**
Cytochrome c	1.02±0.09	0.96±0.15	1.14±0.17	1.08±0.20
Apaf-1	1.00±0.08	1.06±0.13	1.02±0.09	1.12±0.16
Fas	1.05±0.06	1.20±0.19	1.45±0.22*	1.86±0.20**
FasL	1.03±0.10	1.17±0.13	1.64±0.19**	2.05±0.34**

The data are expressed as the mean ± SD for six animals per dose. *$P < 0.05$, **$P < 0.01$ *versus* Vehicle control.

Legends to Figures

Figure 1. Effects of 4-nonylphenol on epididymal sperm morphology. Major morphological changes in spermatozoa: Blue arrowhead, double heads and double tails; Red arrowheads, bent or coiled tails; Green arrowheads, bent or coiled heads; White arrowhead, no-hook head; Black arrowhead, no tail. Magnification: ×200.

Figure 2. 4-Nonylphenol exposure affected the serum hormone and fructose content in rat testis. (A) Effects of 4-nonylphenol on serum FSH level of adult male rats; (B) Effects of 4-nonylphenol on serum LH level of adult male rats; (C) Dose-response relationship between 4-nonylphenol and serum testosterone levels; and (D) Effects of 4-nonylphenol on the testicular content of fructose in rats. Each bar denotes Mean ± S.D. of six rats. *P <0.05, **P <0.01 *versus* group without 4-nonylphenol treatment, one-way ANOVA.

Figure 3. Histological morphology of testes stained with H&E from the 4-nonylphenol-treated and control groups. Testicular cross sections from control rats showing normal seminiferous tubules and spermatogenesis. In the 25 mg/kg 4-nonylphenol group, most of the tubule walls were smooth, and the arrangement of the seminiferous tubule was regular. Testicular cross sections from 4-nonylphenol (50 mg/kg) challenged rats showing degeneration with absence of spermatogenic series in the lumen (indicated by blue diamond) of some seminiferous tubules. In samples from rats treated with 100 mg/kg 4-nonylphenol, spermatozoa in the tubules reduced (indicated by red square), the germ cell layers of the seminiferous tubules were discontinuous (indicated by blue circle), even some sloughed germ cells detached into the tubular lumen (indicated by red arrowhead). Magnification: ×200 (red photos), ×400 (purple photos).

Figure 4. Assessment of oxidative stress in 4-nonylphenol-treated and control groups. (A) Effects of 4-nonylphenol on SOD, GSH-Px and MDA of testicular tissue in rats; and, (B) Effects of 4-nonylphenol on the levels of serum SOD, GSH-Px and MDA in rats. Each bar denotes Mean ± S.D. of six rats. *P <0.05, **P <0.01 *versus* group without 4-nonylphenol treatment, one-way ANOVA.

Figure 5. Effects of 4-nonylphenol on mRNA levels of oxidative stress-related genes in rat testis. (A) Comparison of *SOD1*; (B) Comparison of *CAT*; (C) Comparison of *GPx*; and, (D) Comparison of *CYP1B1*. Each bar denotes Mean ± S.D. of six rats. *P <0.05, **P <0.01 *versus* group without 4-nonylphenol treatment, one-way ANOVA.

Figure 6. Effects of 4-nonylphenol on the ultrastructure of spermatogenic-lineage cells present in seminiferous tubules visualised by transmission electron microscope. (A) spermatogonia; (B) Sertoli cell; (C) Leydig cell; (D) primary spermatocyte; (E) secondary spermatocytes; (F) round spermatids with deposition of chromatin on the superior base toward the sperm formation; (G) spermatids; and, (H) sperm (red arrow). Bar: 2 μm; 1 μm; 0.5 μm. Three rats were randomly selected from each treatment group for ultrastructural evaluation.

Figure 7. 4-Nonylphenol induced proliferation inhibition and apoptosis in the rat testis. (A) Inhibitory effects of 4-nonylphenol on testicular cell-proliferation. Ki-67-positive staining indicative of the proliferative capacity was detected as bright-green fluorescent (×200). (B) Effects of 4-nonylphenol on induction of testicular apoptosis. TUNEL-positive staining indicative of DNA fragmentation was detected as bright-green fluorescent on the nuclei of apoptotic cells (×200).

Figure 8. 4-Nonylphenol induced testicular apoptosis involving the activation of p53-Bcl-2/Bax-Fas signalling pathways. (A) Effects of 4-nonylphenol on the expression of Bax, Bcl-2, Fas, FasL and p53 in testicular tissue. The blots shown are representative of three independent western blots for each rats. (B) Densitometric analysis of the immunoreactive bands. Quantitative data are expressed as mean ± SD. n = 6. The Y axis represents the relative protein expression level (the ratio of target protein/*β-actin* and Bcl-2/Bax). *$P < 0.05$, **$P < 0.01$ *versus* control group without 4-nonylphenol treatment, one-way ANOVA.

Figure 9. Diagram tying together the activation of p53-Bcl-2/Bax-Fas/FasL signalling involved in 4-nonylphenol-induced disruption of spermatogenesis and oxidative stress-related apoptosis.

**Figure 1**
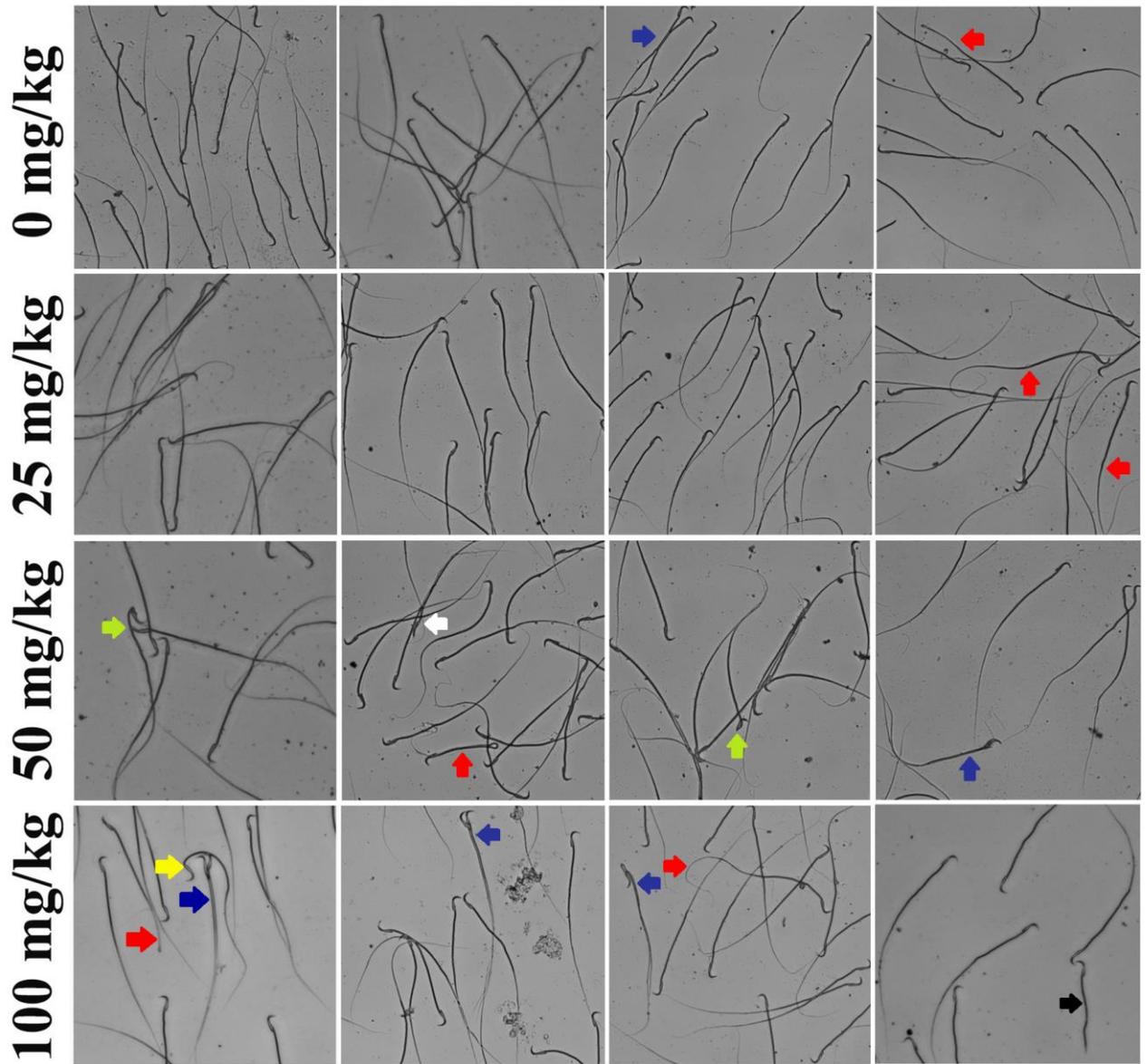
Figure 2
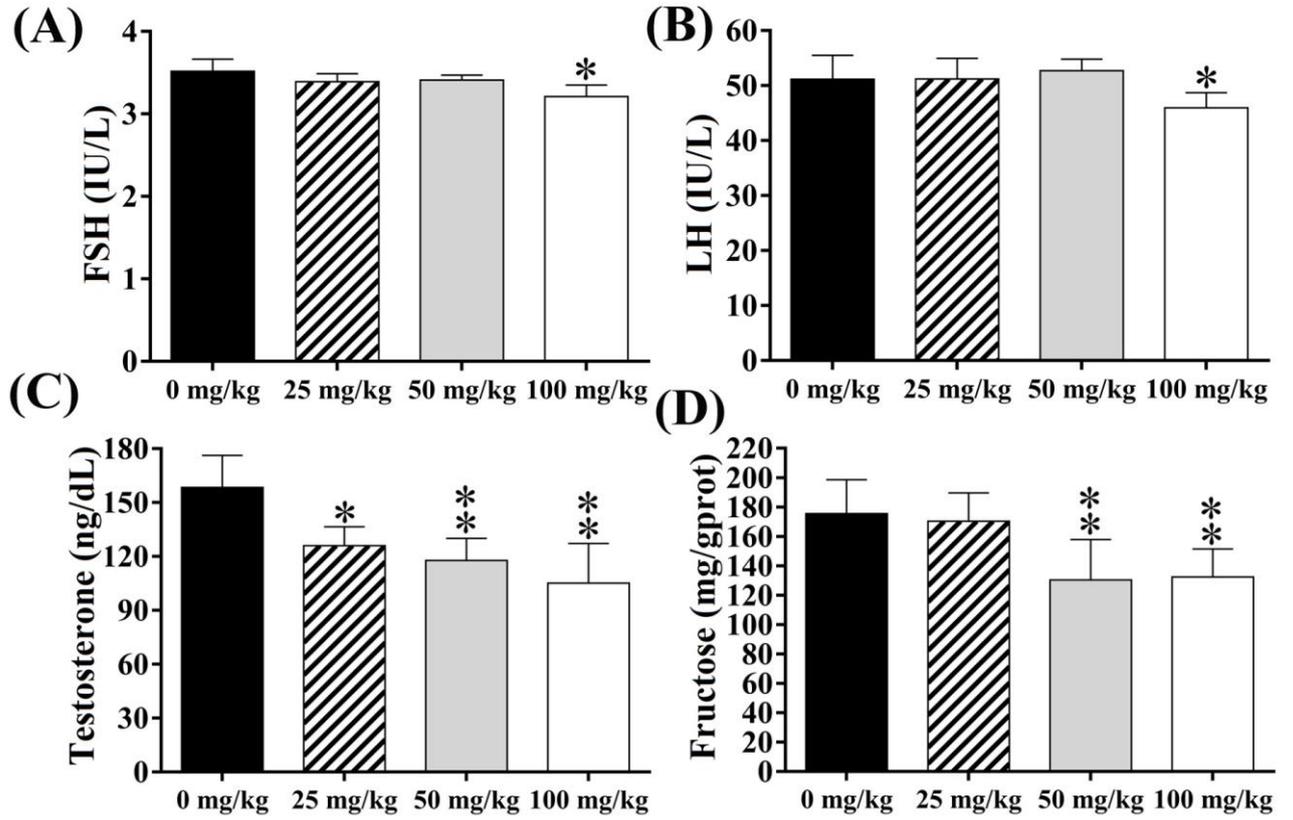
Figure 3
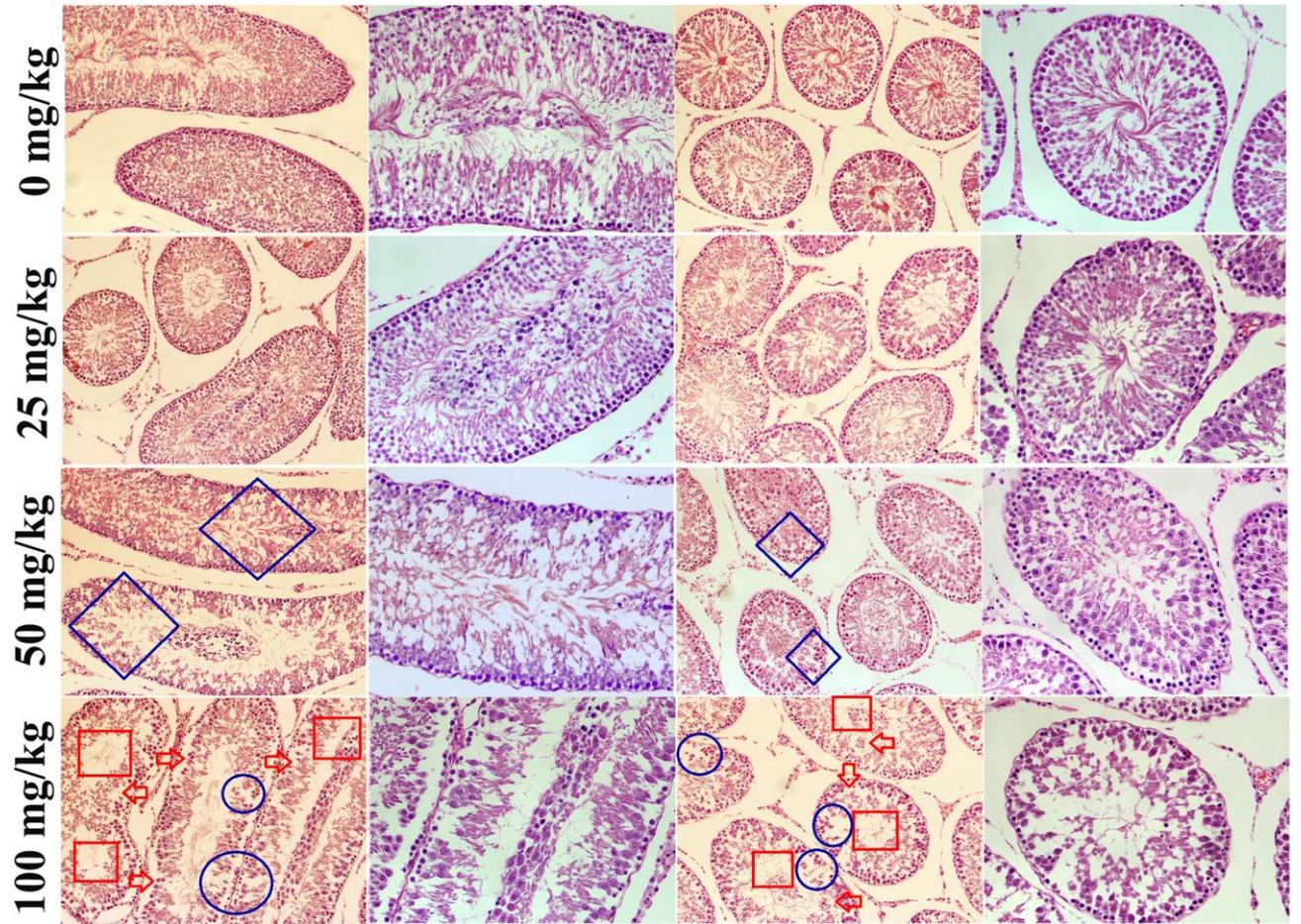
Figure 4
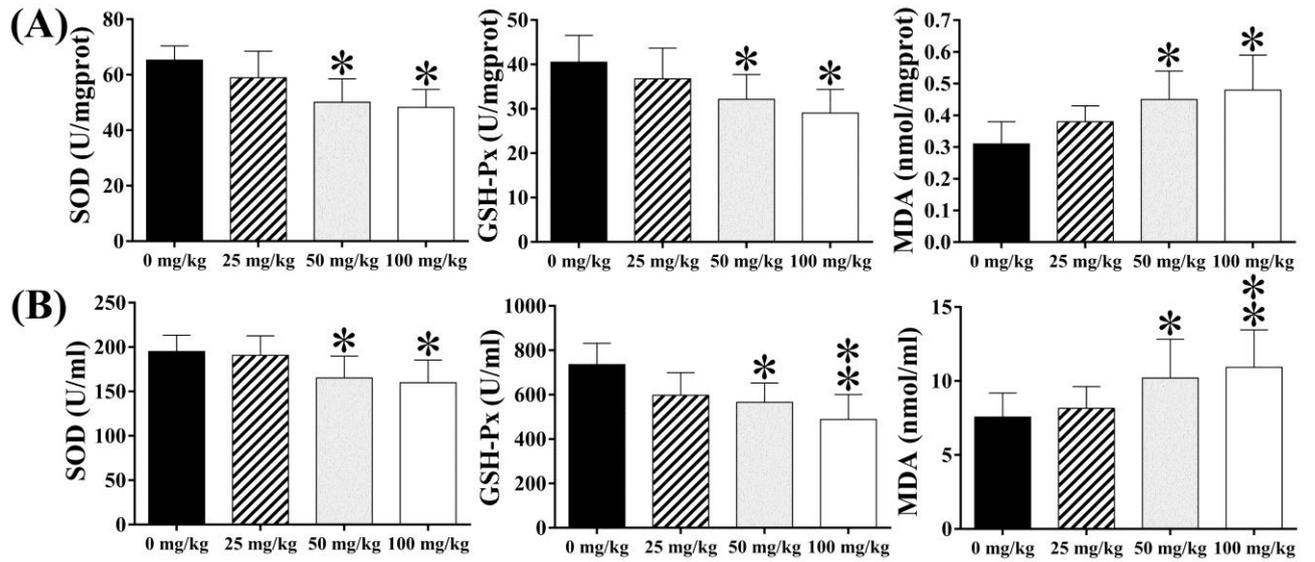
Figure 5
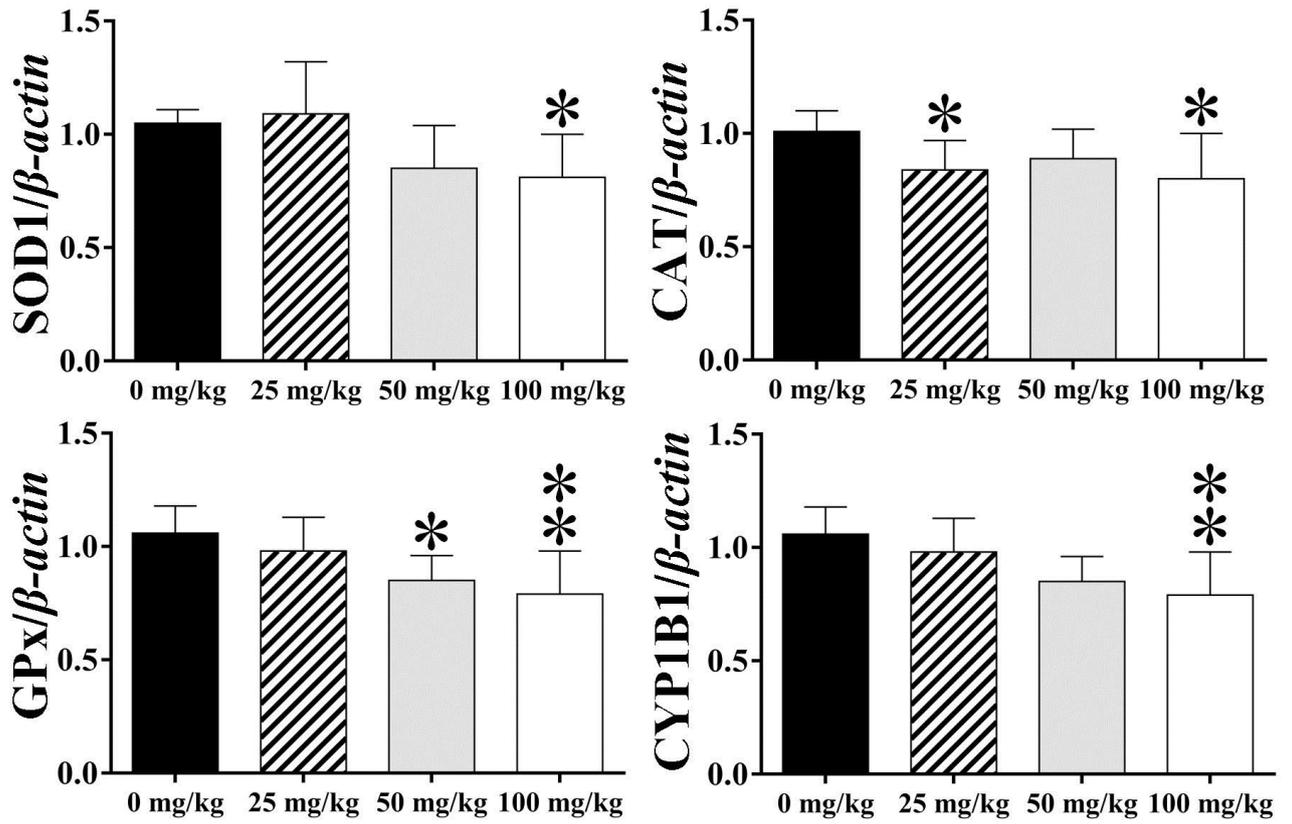
Figure 6
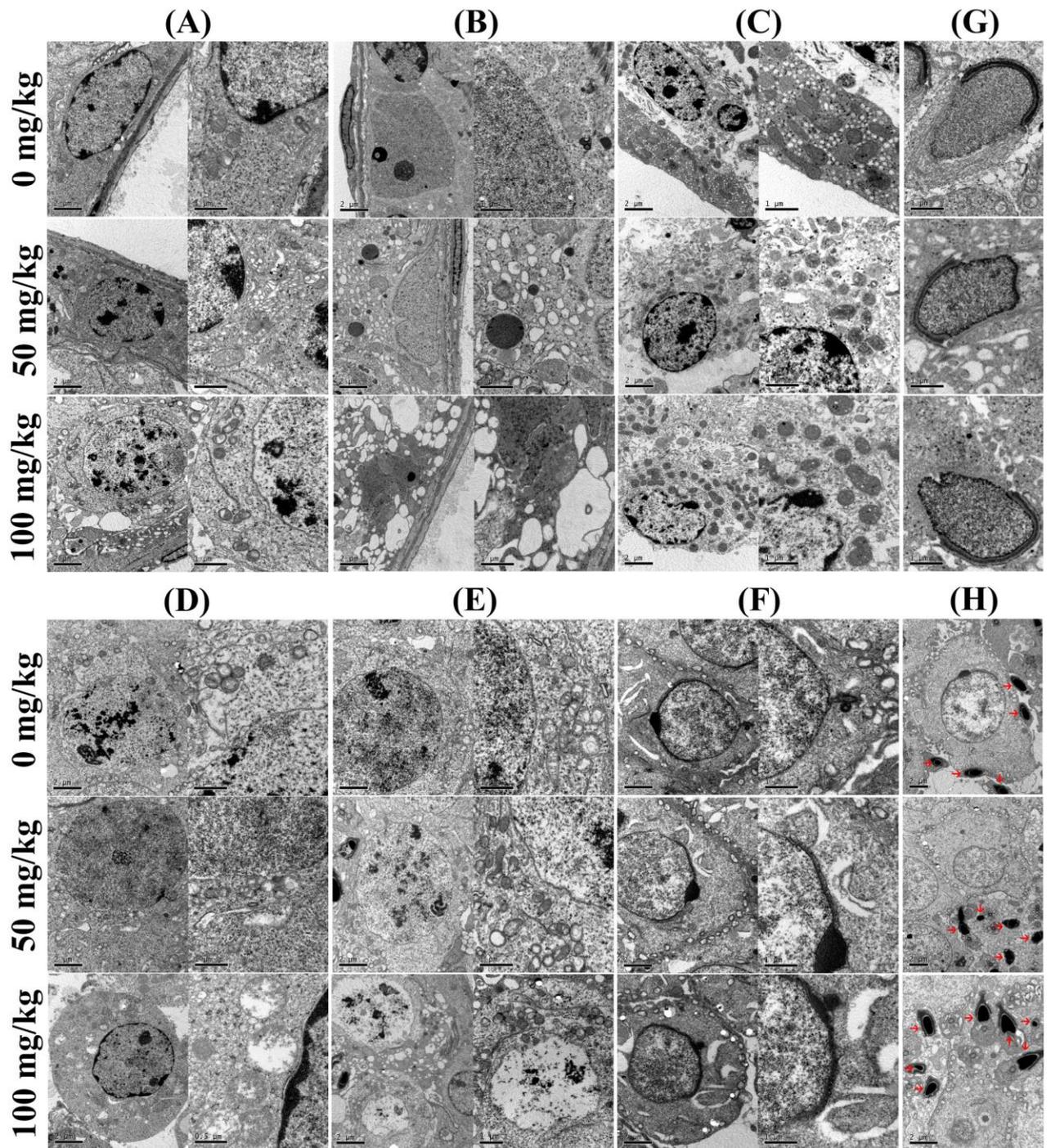
Figure 7
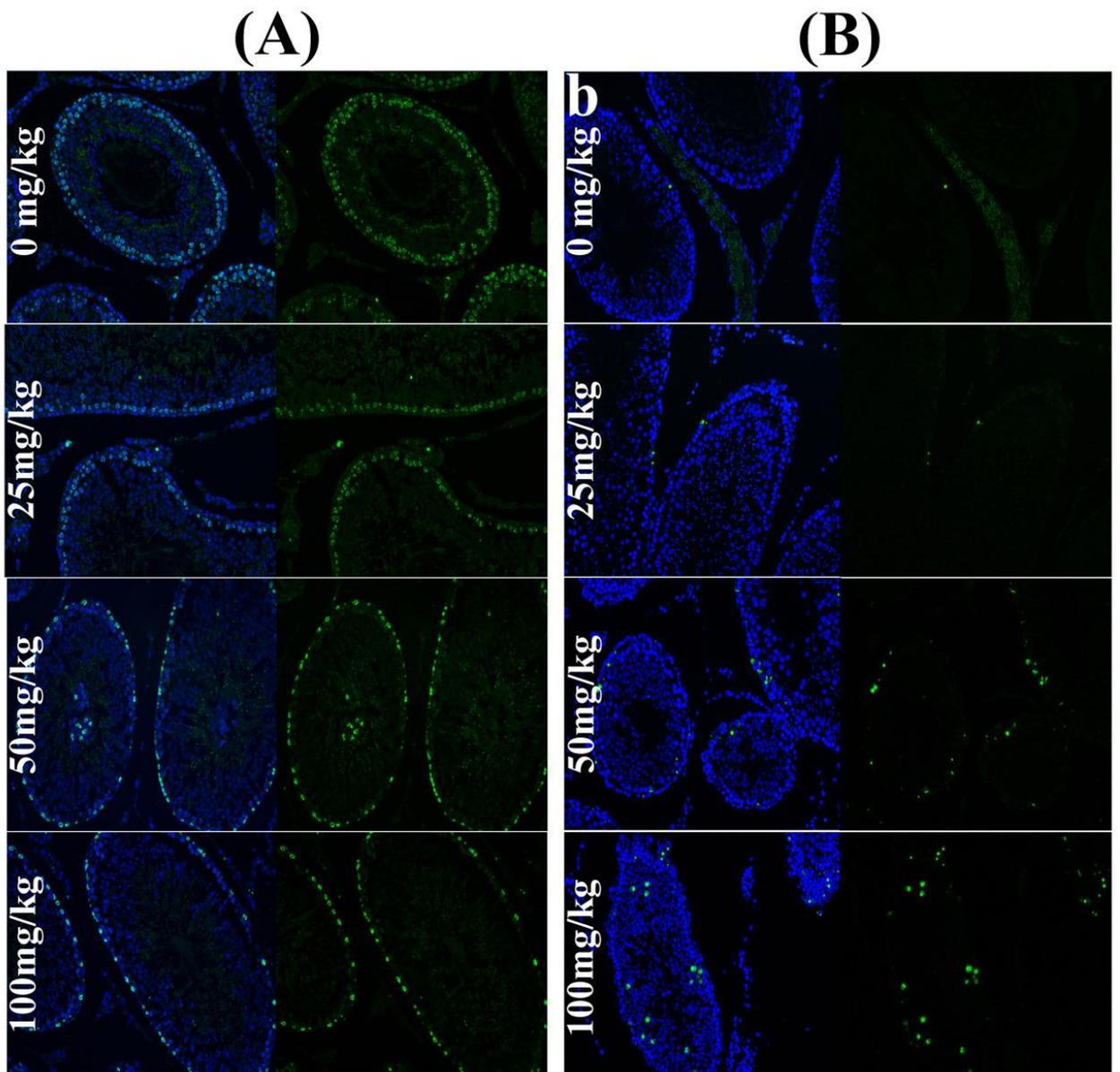
Figure 8
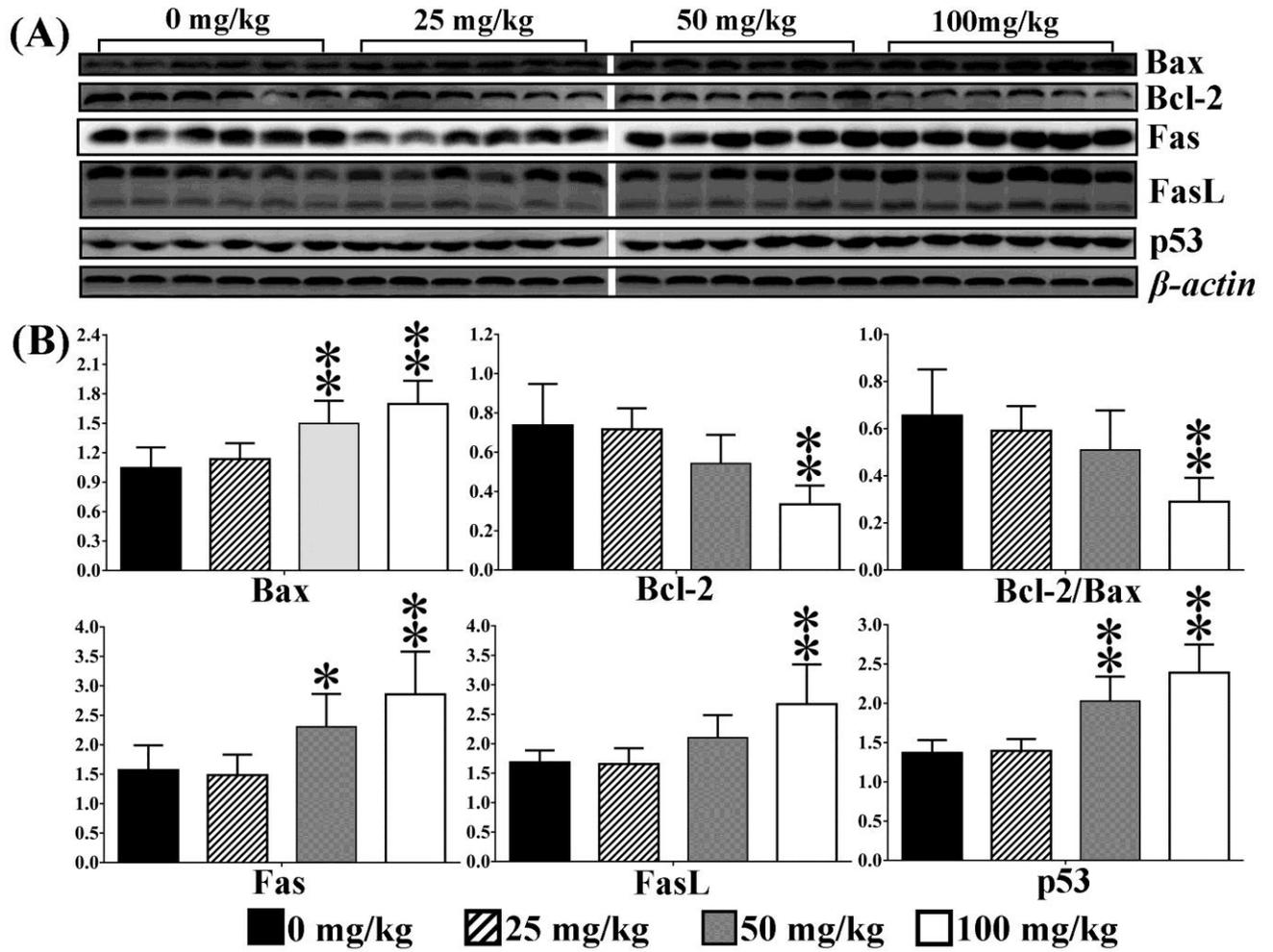
Figure 9
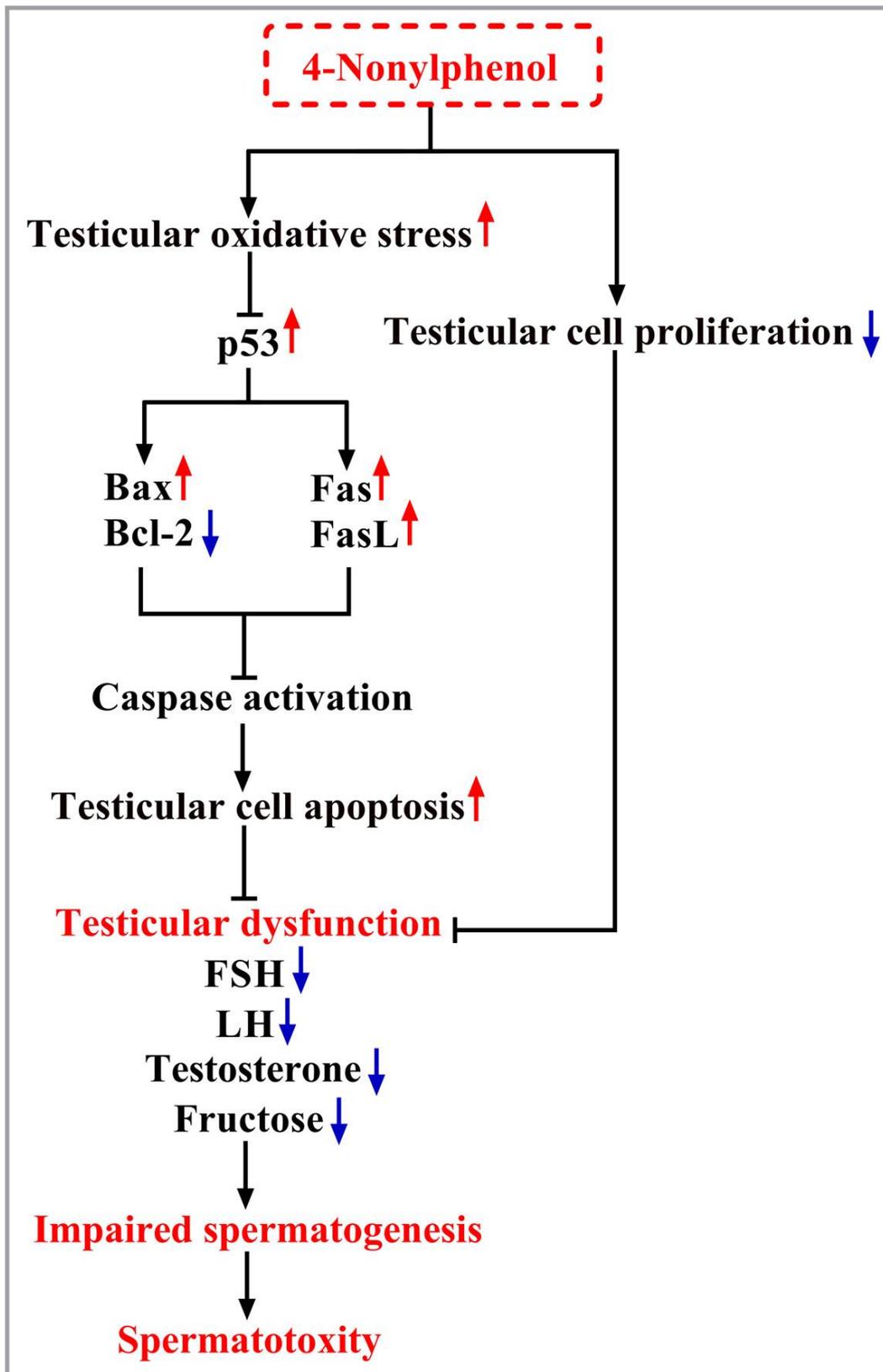
Figure S1
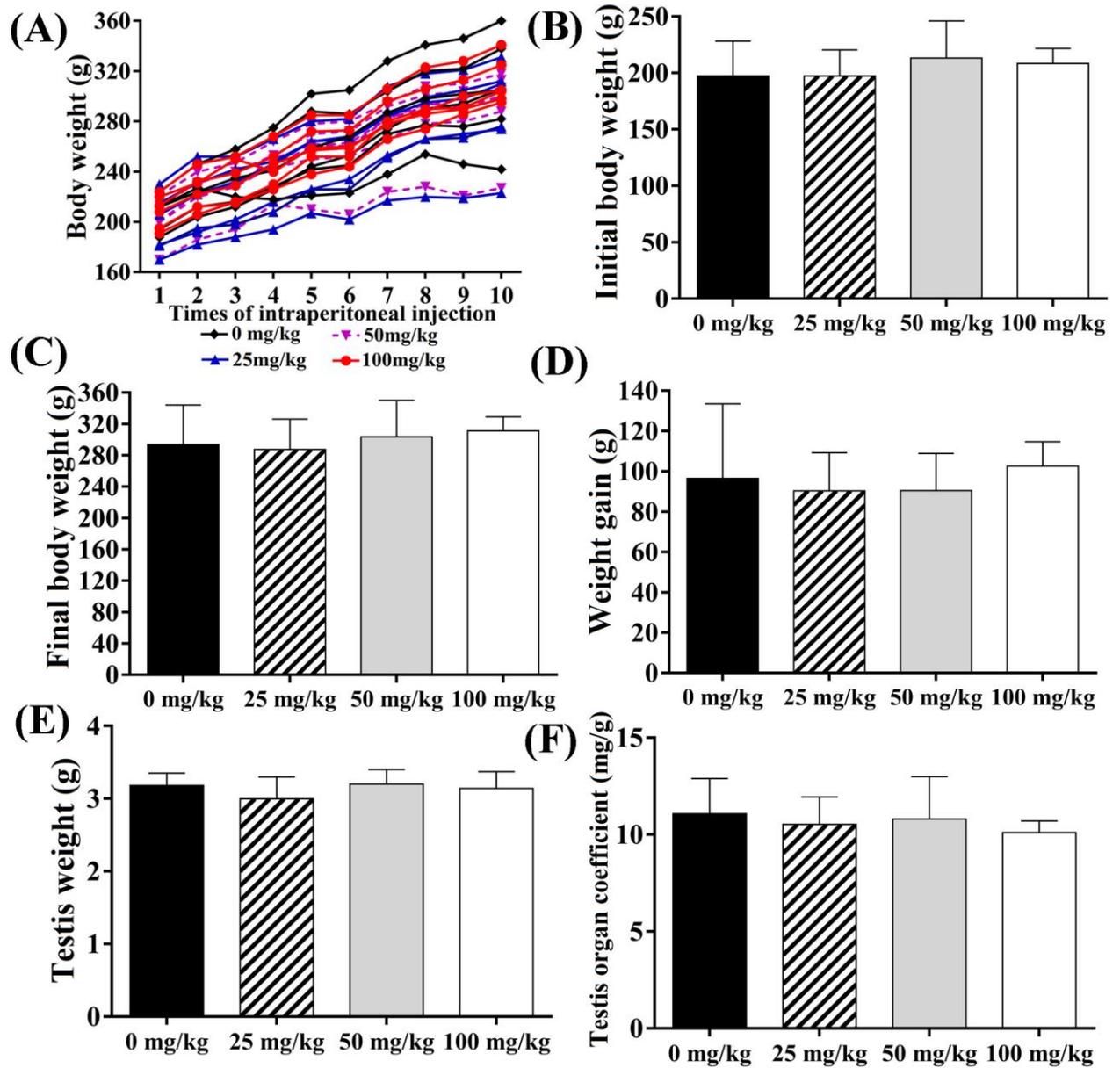
Table S1. Primer sequences used in real-time RT-PCR				
Gene	GenBank Accession numer	Primer sequences (5′-3′)		Length (bp)
		Forward	Reverse	
β-actin	NM_031144.3	GGAGATTACTGCCCTGGCTCCTA	GACTCATCGTACTCCTGCTTGCTG	150
SOD1	NM_000454.4	TGCCGTCCGATTCTCCACAG	CCACATTGCCCAGGTCTCC	103
CAT	NM_001752.3	TGCCGTCCGATTCTCCACAG	TCCCACGAGGTCCCAGTTAC	115
GPx1	XM_005372442.1	GTCCACCGTGTATGCCTTCTCC	TCTCCTGATGTCCGAACTGATTGC	218
CYP1B1	NM_012940.2	GAGCTCGCTGTCTACCCAAC	GATCTGAAAAACGTCGCCAT	223
Caspase-1	NM_012762.2	AAGGTGGCGCATTTCCTGGAC	GGGCACTTCAATGTGTTCATC	448
Caspase-2	XM_006236394.2	ATGCTAACTGTCCAAGTCTA	GTCTCATCTTCATTAATTCC	168
Caspase-3	XM_006253130.2	GGTATTGAGACAGACAGTGG	CACGGGATCTGTTTCTTTGC	281
Caspase-6	XM_008761527.1	GGAGACAAGTGTCAGAGCCTG	CGTTCACAGTCTCTCGGTGAG	241
Caspase-7	XM_008760550.1	GAAGTGACTGTCTATAATGAC	TGCCATGCTCATTCAGGATGG	442
Caspase-8	XM_006245015.2	GCTCTCCTACCCCTTGGTAAG	AACCCTGTAGGCAGAAACCTG	331
Caspase-9	NM_015733.5	TGCACTTCCTCTCAAGGCAGGACC	TCCAAGGTCTCCATGTACCAGGAGC	206
Caspase-11	AY029283	CTTCACAGTGCGAAAGAACTG	GAGTCCACATTAAGAAATGTC	275
Bax	XM_011250780.1	CAGGATGCGTCCACCAAGAA	CGTGTCCACGTCAGCAATCA	102
Bad	XM_006230896.2	GCCCTAGGCTTGAGGAAGTC	CAAACTCTGGGATCTGGAACA	109
Bcl-xl	XM_006498611.2	GGTGAGTCGGATTGCAAGTTG	CCGCCGTTCTCCTGGAT	75
Bcl-2	NM_016993.1	GGGATGCCTTTGTGGAACTATATG	TGAGCAGCGTCTTCAGAGACA	81
PCNA1	NM_022381.3	CCGGGACCTTAGCCATATTG	TCACCCCGTCCTTTGCA	59
p53	XM_008767773.1	TTCCCTCAATAAGCTGTTCTGCC	TGCTCTCTTTGCACTCCCTGG	538
Cytochrome c	XM_003753058.3	GGCAAGCATAAGACTGGACCAA	TTTCCAAATACTCCATCAGGGTATC	139
Apaf-1	XM_008765263.1	GATATGGAATGTCTCAGATGGCC	GGTCTGTGAGGACTCCCCA	184
Fas	XM_011247141.1	ACATGGACAAGAACCATTATGCTGA	CTGGTTTGCACTTGCACTTGGTA	123
FasL	XM_006496654.2	GGAATGGGAAGACACATATGGAACTGC	CATATCTGGCCAGTAGTGCAGTAATTC	237